Laser-induced phenomena at liquid-glass interfaces: Particle deposition and holographic bubble grating formation

Gregory Eyring and M. D. Fayer
Department of Chemistry, Stanford University, Stanford, California 94305

(Received 11 July 1983; accepted for publication 30 September 1983)

Intense diffraction from a periodic array of microscopic bubbles is reported. These bubble gratings are generated by 100-ps, 1.06-μm pulses of intensity 10^8–10^9 W/cm^2 which are crossed at a liquid-dielectric interface. The time dependence of the diffraction yields information on the surface bubble expansion, contraction, and migration. It is demonstrated that there is a mechanism by which optical radiation can transfer impurity particles from the liquid to the glass surface. These surface particles are strongly heated by subsequent laser pulses, causing them to produce bubbles. Laser-induced particle deposition also lowers the threshold for surface damage. Once attached, the particles can be removed from the surface using a double pulse sequence with pulse separations $\leqslant$30 ns. This desorption process is related to the temperatures and cooling rates of the surface particles, which can be estimated by analyzing the spectral and temporal characteristics of the emitted blackbody radiation. The dependence of these phenomena on the laser intensity and the chemical properties of the liquid is described, and a variety of possible applications are discussed.

PACS numbers: 79.20.Ds, 78.20.Nv

I. INTRODUCTION

In this paper we describe and analyze novel phenomena observed when the interface between glass or quartz and certain liquids is repeatedly exposed to subnanosecond laser pulses of intensity 10^8–10^9 W/cm^2. Our results demonstrate that there is a mechanism by which optical radiation causes impurity particles from the liquid to be deposited on the glass surface. This deposition can be readily observed with a light microscope at 100$\times$ magnification. These surface particles are strongly heated by subsequent laser pulses, causing them to give off light and to generate bubbles. The spectrum of the emitted light has the form of a blackbody curve, and this was used to estimate the distribution of particle temperatures, while the time dependence of the emission decay served to characterize their cooling rates.

If the surface is exposed to the interference pattern produced by a pair of crossed excitation pulses, bubbles are nucleated selectively in the intensity peaks of the interference fringes, giving rise to bubble gratings.[1] Because of the large difference in refractive index between the gas and liquid, these bubble gratings, though very thin ($\sim$1 μm), result in efficient diffraction of a variably delayed probe pulse brought in at the Bragg angle. By examining the dependence of this diffraction on probe pulse decay between 10^{-10} and 10^1 s, a variety of dynamical properties of the surface bubbles can be studied. These are the expansion, contraction, and migration of the bubbles on the surface.

By bringing in a second set of grating excitation pulses collinear with, but a short time (nanoseconds) after the first set, it was possible to remove the particles attached to the surface and eliminate the probe pulse diffraction. This desorption effect was studied as a function of delay time between sets of excitation pulses, and was found to be related to the particle cooling rate.

The presence of dust particles in samples and on optical surfaces has long been a concern of the spectroscopist who uses high peak power pulsed lasers. Light-absorbing impurities can greaty reduce the threshold for surface damage on optics, and in samples they can obscure or interfere with experimental results. For example, the emission of charged particles and visible light from the surfaces of optical cell windows following an intense laser pulse was originally attributed to an intrinsic property of dielectric materials, but it was later found to be primarily due to thermionic emission from hot dust particles attached to the surface.[2–4] In bulk liquids, laser-heated impurity particles produce bubbles which cause scattering and refraction of the laser pulse.[5–11] Such effects are not observed when pulse powers are reduced or when cw beams are used.

In view of the importance of dust particles in liquids exposed to high power laser pulses, it is particularly intriguing that these particles can be transferred from the bulk to the surface in a pattern determined by the laser intensity distribution at the interface. Once attached to the surface these particles can be involved in novel phenomena such as the generation of microscopic bubble diffraction gratings. Our results also suggest that laser-induced particle deposition can play an important role in promoting surface damage at glass-liquid interfaces.

II. EXPERIMENTAL MODELS

The laser system used in these experiments is diagramed in Fig. 1. A continuously pumped Nd:YAG oscillator is acousto-optically mode locked and Q switched to produce 1.06-μm pulses at 400 Hz.[12] The output is a train of some 40 mode-locked pulses, $\sim$100 ps wide and separated by 9 ns. An $\sim$50-μJ pulse from the center of the train is selected by a Pockels cell. In some experiments, an addi-

 0021-8979/84/114072-09$02.40

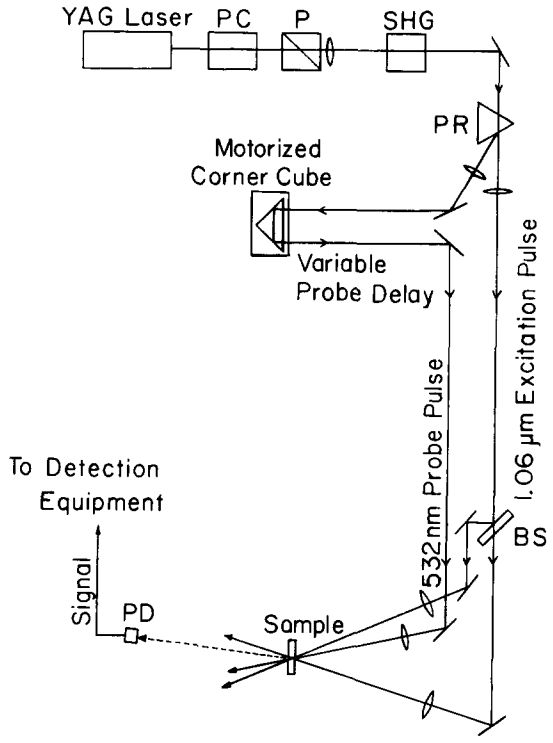

FIG. 1. Nd:YAG laser system used to excite and probe the liquid-glass interfaces. A single 100-ps, 1.06-μm pulse is selected from the mode-locked pulse train and a small portion is frequency doubled to give a 532-nm probe pulse. The remainder is beamsplit and recombined at the interface to give the grating excitation. The grating is probed at the Bragg angle by the 532-nm pulse after it passes down a variable optical delay line. The diffracted part of the probe pulse is detected by a photodiode coupled to either a lock-in amplifier or a waveform recorder. Abbreviations: PC≡Pockels cell; P≡polarizer; SHG≡second harmonic generator; PR≡prism; BS≡beamsplitter; PD≡photodiode.

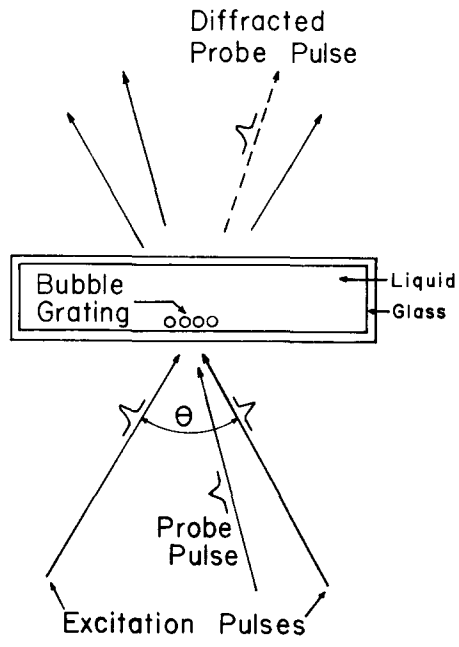

FIG. 2. Schematic illustration of the experimental geometry for the production and detection of bubble gratings. Two 100-ps, 1.06-μm excitation pulses are crossed at the interface between a glass cuvette and a liquid. Stripes of microscopic bubbles are generated in the intensity peaks of the resulting interference pattern. This bubble grating causes strong diffraction of a variably delayed, 532-nm probe pulse brought in at the Bragg angle.

tional Pockels cell was used to select out a subsequent pulse from the train. In this way, double pulse sequences could be obtained with the time delay between pulses equal to any desired multiple of the 9-ns pulse interval, from 9 to 99 ns.

A small portion of the IR single pulse is frequency doubled using CD*A to give an ~ 1-μJ probe at 532 nm. The remainder is beamsplit to give two ~ 15-μJ pulses which, after traveling equal path lengths, are crossed at an angle θ at the interface between a glass or fused silica cell and a liquid (Fig. 2). The interface is thus exposed to a sinusoidally varying pattern of intensity peaks and nulls produced by the interference between the IR excitation beams. The fringe spacing is given by

$$\Lambda = \frac{\lambda}{2\sin(\theta/2)}, \tag{1}$$

where λ is the laser wavelength. In a typical case, $\theta = 26°$, $\lambda = 1.06\,\mu$m yields a value of $2.36\,\mu$m for Λ.

The interaction region of the IR beams is probed at the Bragg angle with a 532-nm pulse which could be timed to arrive continuously from 2 ns before to 16 ns after the IR excitation, using an optical delay line. In cases where longer excitation-probe delays were required, an argon-ion pumped cw dye laser was used as a probe. Spot sizes of the excitation and probe beams were 100 and 50 μm, respectively. Most of our measurements were carried out on benzyl benzoate in a 1-mm absorption cuvette, but this was largely a matter of convenience, since intense diffraction was observed in several other liquids, and in the isotropic phases of several liquid crystals. The dependence of the effect on particular types of liquids is discussed below.

The probe diffraction was detected by a photodiode coupled to a lock-in amplifier or a Biomation model 805 waveform recorder. The spectrum of the visible light emitted following excitation by a double pulse sequence of two identical IR pulses separated by 9 ns was recorded using a computer-interfaced SPEX 1-m monochromator equipped with a Hammamatsu No. 928 phototube. The spectrum was corrected for phototube and grating response using a blackbody lamp as a standard. The time dependence of the visible light emission was obtained using a fast phototube and a Tektronix R7912 transient digitizer.

III. RESULTS AND DISCUSSION

A. Bubble gratings

Our original observation of bubble gratings occurred in samples of liquid crystals which were subjected to the crossed beam excitation (Fig. 2). Typical results for the isotropic phase of the nematic liquid crystal *p-p'* pentylcyanobiphenyl (5-CB) are shown in Fig. 3. The data are the output of a lock-in amplifier. At $t = 0$ a fresh sample spot was exposed to the crossed IR excitation and green probe pulses. The excitation and probe repetition rate was 400 Hz. At first, no probe diffraction could be observed. After one to two minutes, however, a first order diffraction spot appeared which rapidly increased its intensity over ~ 15 s until it reached a few percent of the transmitted probe intensity. The onset time was independent of whether the probe delay was a few

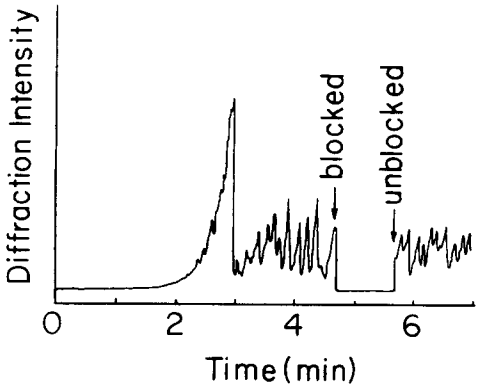

FIG. 3. Time course of the diffracted probe intensity for the isotropic phase of the liquid crystal 5-CB. At $t = 0$, the crossed excitation beams are turned on. After an ~2-min onset time, the first order diffraction intensity increases to several percent of the undeflected probe beam. Thereafter, it rises and falls erratically as long as the excitation beams are present. If the excitation beams are blocked, the diffracted intensity is zero. When the excitation beams are unblocked, diffraction is observed immediately, without the 2-min onset time. This result is independent of the length of time during which the excitation beams are blocked.

nanoseconds or a few milliseconds relative to the excitation. At this point the diffraction fell sharply to a low (nonzero) value, and, if exposure to the IR beams was continued, the diffraction intensity rose and fell at ~15-s intervals indefinitely. Blocking either of the excitation beams (arrow) caused the probe diffraction to drop rapidly to zero. When the excitation beams were unblocked (arrow) diffraction was observed immediately without the 1–2-min buildup time. This occurred whether the IR beams were blocked for a few minutes or a few days.

When the sample was translated more than one spot diameter to the right or left, no diffraction could be seen for at least a minute. After returning to the original spot, however, intense diffraction was observed immediately. Thus, the sample "remembered" where it had previously diffracted light. Furthermore, the region several spot diameters *above* the orignal spot also gave immediate diffraction, even though it had never been exposed to the excitation beams. The same effect was not observed below the original spot. The memory was not a grating in itself since no diffraction was observed when only the probe beam was present. Instead, it consisted of a tendency, or "predisposition," to form a grating very rapidly when the crossed excitation beams were turned on. The predisposed region of the surface was associated with a dark residue of material which was visible under a light microscope (see Sec. C below). The surface could be predisposed with a single beam, but the crossed excitation beams were required to observe diffraction.

The onset time of the diffraction from a fresh sample spot increased as the laser repetition rate was reduced, but diffraction was always observed eventually, even below 100 Hz. In contrast, if the excitation intensity were cut in half with a neutral density filter, diffraction was never observed. Thus, the effect depended on peak power rather than average energy, with a threshold in the vicinity of 10^8 W/cm^2 under our conditions.

A closer examination of the sample by a 100× magnification microscope revealed that the abrupt drops in probe diffraction displayed in Fig. 3 corresponded with the release of an ~40-μm-diam bubble from the surface of the glass at the laser spot. These bubbles were stable for minutes, and, once released, floated slowly to the surface of the liquid. This observation implies that a grating of microscopic bubbles is the origin of the diffraction. The grating thickness can be estimated assuming that a large bubble is released when the smaller bubbles approach uniform coverage of the laser spot. For the observed 40-μm-diam bubble and a spot size ~100 μm, one obtains a diameter ~1 μm for the microbubbles. This estimate is consistent with the diffusion measurements discussed below. The large difference in refractive index $\Delta n = 0.3$–0.6 between gas or vapor and liquid accounts for the relatively high diffraction efficiency (up to 10% in the + 1 order) from a grating only 1 μm thick.

The nature of the diffracted light was examined more quantitatively using a fast *pin* photodiode and a Biomation model 805 waveform recorder. The character of the diffraction from a predisposed spot was found to be dramatically different depending on whether the grating was probed a few nanoseconds or a few milliseconds after the arrival of the excitation pulses. The millisecond delay was achieved by adjusting the optical delay line so that the probe arrived at the sample slightly before the excitation pulses (i.e., 2.5 ms after the previous excitation pulse for a 400-Hz repetition rate). Figure 4(a) displays the diffracted light intensity of a series of shots for the case where the grating was probed 1 ns after the

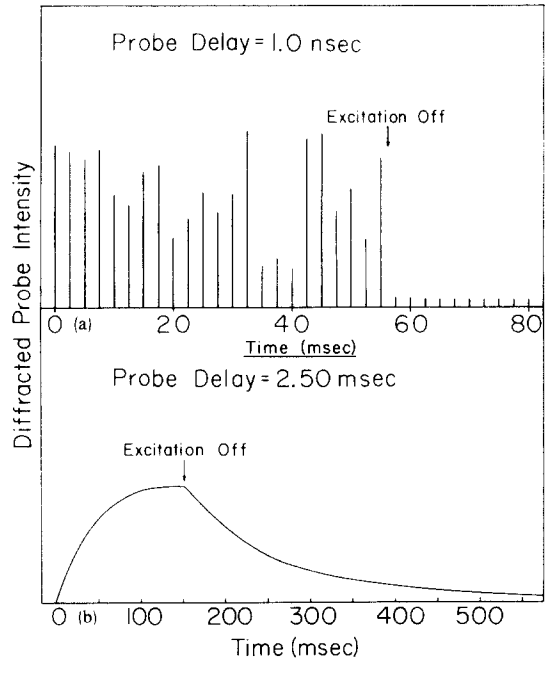

FIG. 4. Time course of the diffracted probe intensity at a predisposed spot on the glass-liquid interface when the bubble grating is probed 1 ns (a) and 2.5 ms (b) after the arrival of the crossed excitation pulses. The excitation pulses are turned on at $t = 0$ and blocked at the arrows. Each spike in (a) corresponds to an individual laser shot (400 Hz). The vertical scale in (b) is expanded by a factor of 10 relative to (a). Since in (b) the shot-to-shot fluctuation in the diffraction is small, only the envelope of the diffracted probe pulses is depicted.

excitation of a predisposed spot. Intense diffraction was observed on the first shot and continued erratically until the excitation beams were blocked (arrow), after which a large fraction of the intensity disappeared before the next probe shot 2.5 ms later.

A very different behavior was observed when the grating was probed 2.5 ms after the arrival of the excitation, as shown in Fig. 4(b). The overall first order diffraction efficiency was an order of magnitude weaker, so the vertical scale is expanded by a factor of 10 relative to Fig. 4(a). The time scale has been contracted in order to show the behavior of the grating long after the excitation beams are blocked. The diffraction is much more stable from shot to shot so only the envelope of the diffracted probe pulses is shown. The intensity takes 15–25 shots to build up to a steady state level. When the excitation beams are blocked (arrow), the intensity decays exponentially to zero over several hundred milliseconds.

These data are readily explained by a laser-induced bubble grating model as follows. The excitation pulses are partially absorbed by small particles attached to the surface which lie in the grating peaks. This local heating vaporizes and degasses the surrounding liquid producing a grating of expanding bubbles containing both vapor and noncondensable gas. The presence of these hot, expanded bubbles gives rise to the intense and erratic diffraction Fig. 4(a). After a time short compared with the repetition rate, the vapor condenses, leaving smaller residual gas bubbles having a lifetime of many seconds. These smaller bubbles are responsible for the diffraction in Fig. 4(b). The formation of gas bubbles results in depletion of dissolved gas at the interface, which is replenished by diffusion of gas molecules from the surrounding liquid. Thus, the gas bubble production rate reaches a steady state value after 15–25 shots.

When the excitation beams are blocked [Fig. 4(b)], the concentrations of microbubbles in the peaks and nulls become equal by migration of the bubbles on the surface. If this migration corresponds to simple diffusion, the diffraction intensity will decay exponentially with a time which depends on the fringe spacing[13]:

$$I(t) = I_0 \exp\left[-2\left(\frac{2\pi}{\Lambda}\right)^2 Dt \right], \tag{2}$$

where D is the bubble diffusion constant. Measurements of these decays at different fringe spacings should result in different decay rates, but the same diffusion constant. In Fig. 5, the decays observed at two fringe spacings are plotted. Within experimental error, these yield the same value for $D = 1.8 \pm 0.6 \times 10^{-9}$ cm^2/s. The fact that both decays are exponential suggests that the microbubbles are relatively uniform in size.

From kinetic theory, the diffusion constant of a particle undergoing Brownian motion is

$$D = \frac{6KT}{f}, \tag{3}$$

where f is the friction coefficient. For a spherical particle of radius r immersed in a medium of viscosity η, f is given by Stokes' equation:

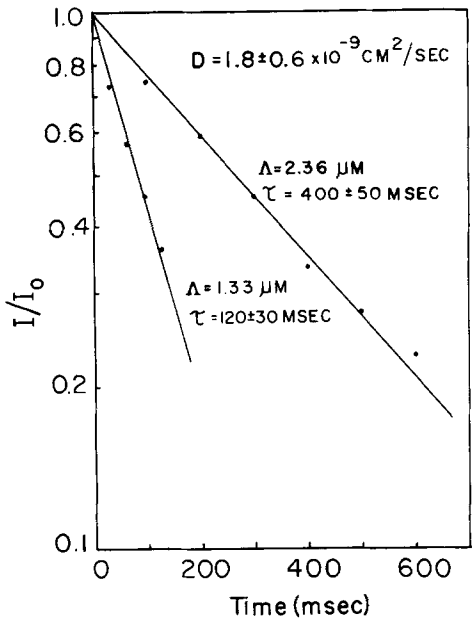

FIG. 5. The intensity of the + 1 order probe diffraction vs time after blocking the excitation beams. The points are taken from curves like that in Fig. 2(b) (following the arrow) for two different values of the fringe spacing Λ. Both decays are exponential and, while their time constants τ are very different, the calculated diffusion constant D is the same. This demonstrates that the loss of diffracting power is due to the diffusion of microscopic gas bubbles from the grating peaks to the nulls.

$$f = 6\pi\eta r. \tag{4}$$

If we neglect the interaction of the bubbles with the surface, these formulas can be used to verify that the bubble diffusion constant measured above is the right order of magnitude. Taking $T = 300$ °K, $\eta = 8.5 \times 10^{-2}$ P for benzyl benzoate, and r in the range 0.1–1 μ, we obtain D in the range 10^{-8}–10^{-9} cm^2/s. This agrees well with our experimental value.

The maximum possible diameter of the microbubbles is the grating fringe spacing Λ. The data shown in Fig. 5, however, suggest that their actual size is independent of Λ, since the diffusion constant which varies inversely as the bubble radius [Eqs. (3) and (4)] was the same for the two different fringe spacings. Thus, the smaller value of $\Lambda = 1.33$ μm gives an upper limit to the diameter of the microbubbles.

The onset and decay times of the intense, erratic diffraction were determined in separate experiments. The time delay between the point when the probe and excitation beams were simultaneously present at the interface ($t = 0$) and when the intense diffraction was observed, was measured with the optical delay line to be 350 ± 50 ps. This is roughly the time which would be required for a bubble expanding at the speed of sound in benzyl benzoate ($\sim 2 \times 10^5$ cm/s) to reach a radius of 1 μm.

In order to measure the loss of diffraction efficiency caused by the collapse of the hot bubbles, it was necessary to probe the grating with a cw beam so that diffraction could be followed continuously on a microsecond time scale. For this purpose we used an ~50-mW, 590-nm beam from an argon-ion pumped rhodamine-6G dye laser as a probe. The time course of the diffraction from a single shot of the IR grating

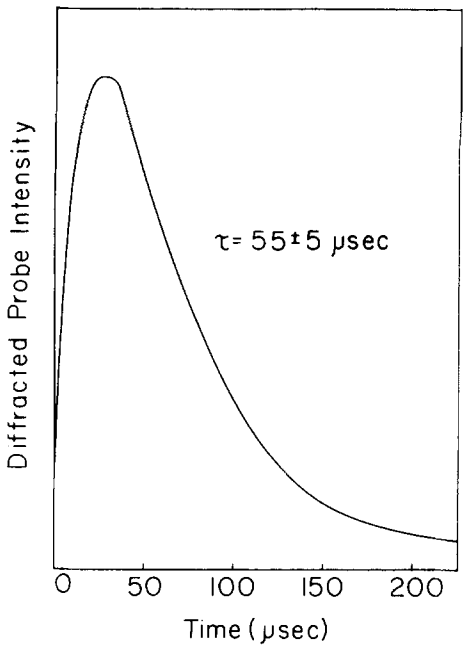

FIG. 6. First order diffraction of a cw probe beam vs time following a single shot of the IR grating excitation on a predisposed spot. The true rising edge (350 ps) is not resolved in this experiment. The decay time is $55 \pm 5\,\mu$s. This reflects the time required for the hot, expanded bubbles to cool and contract.

is shown in Fig. 6. For these experiments, the recording instrument risetime was $\sim 4\,\mu$s. Therefore, the 350-ps rising edge of the diffraction is not resolved. The decay is approximately exponential with a time constant of $55 \pm 5\,\mu$s. We propose that this is the time required for the expanded bubbles to contract by the loss of heat to the surroundings, causing the vapor to condense.

B. Suppression of diffraction with a double pulse sequence

Once a spot on the interface had been predisposed to diffract light with IR single pulses, we found that we could reversibly suppress the diffraction by switching to a pulse sequence formed by selecting two adjacent pulses from the mode-locked IR pulse train. That is, by changing back and forth between a set of crossed pulses and two sets of crossed pulses separated by 9 ns, we could alternately create and erase the tendency to diffract light.

The erasure does not occur immediately, but over a period of 15–30 s. Diffraction could then be regenerated in the usual time ~ 1 min with the single pulses. A fresh sample spot exposed only to the double pulse sequence neither diffracts light nor produces any visible bubbles. Thus, it is not possible to predispose a spot on the interface when the adjacent pair pulse sequence is used. When we used this double pulse sequence with filters to reduce the intensity to half, no predisposition could be achieved, nor could previous predisposition be erased. The full intensity of the IR pulses is thus required, both to predispose with a single pulse and to erase with a double pulse. At $\sim 10^8$ W/cm^2, we are apparently within a factor of 2 above the intensity threshold for both effects.

These observations show that diffraction behavior depends strongly on the separation time between sets of crossed excitation pulses. A single set followed by another 2.5 ms later (400-Hz repetition rate) constituted the original conditions under which we observed predisposition and strong diffraction. However, two sets of crossed IR pulses separated by 9 ns erased both predisposition and diffraction.

In order to determine the pulse separation at which one type of behavior changed over to the other, we used a second Pockels cell to select out pairs of single pulses from the IR pulse train having various time separations. For a pulse separation of 18 ns, we observed the same behavior as for the 9-ns delay. However, at 27 ns and longer delays, the qualitative behavior began to change, and diffraction was reproducibly seen after onset times in the 4–5 min range. Thus, a second IR pulse only suppressed the diffraction if it arrived within ~ 30 ns after the first. A possible mechanism for this effect is described below.

C. Visible light emission and particle deposition and removal

After prolonged irradiation of the sample by the excitation beams, we could detect a faint dark residue on the glass surface under a microscope. The residue has the form of a round spot with a narrow streak extending upward for several spot diameters. It is clearly the origin of both the diffraction and the bubbles, since when the spot or streak is translated through the crossed beams, a burst of bubbles and diffraction result. Evidently, the rising bubbles carry particles up the surface of the glass from the initial point of deposition in the laser spot, producing the streak.

With the probe beam blocked and the room darkened it is possible to see a very faint emission of visible light upon IR laser irradiation of spots at the glass-liquid interface which had been predisposed. For a fresh spot on the surface, this emission is not observed immediately, but has an onset time corresponding to that for diffraction. We observe the light emission whether our samples were excited with crossed IR beams or a single beam. Like the diffraction, light is emitted immediately when the IR beam is moved several spot diameters above the initial predisposed spot, but not to the right, left, or below. It is therefore associated with the same spot and streak of dark material which is responsible for the diffraction predisposition. Reduction of the IR intensity by a factor of 2 extinguishes the light.

When viewed under a microscope, the spatial profile of the light intensity emitted from a spot predisposed with single pulse excitation reflects the Gaussian profile of the laser. However, excitation of a predisposed spot by a double pulse sequence having 9-ns separation, while increasing the overall emitted light intensity somewhat, causes the spatial profile to change dramatically. The light now appears to come from a bright ring which surrounds a dark central spot. This occurs because particles are removed from the center of the spot under these conditions.

A spectrum of the light emitted from the surface of a quartz cell containing benzyl benzoate following this IR pulse pair excitation is shown in Fig. 7. The spectrum has the

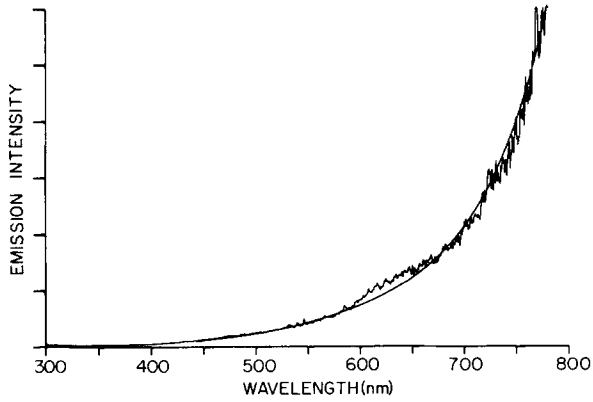

FIG. 7. Spectrum of light emitted by surface particles which were excited by a double pulse sequence with 9-ns time separation between pulses. The solid line is a linear combination of blackbody emission curves for temperatures of 3000 and 1000 °K, with coefficients of 0.35 and 0.65, respectively. The scaling of the composite curve was adjusted to give the best visual fit to the data.

form of a long, smooth tail in the visible which rises steeply toward infrared wavelengths, and strongly resembles a blackbody radiation curve. For purposes of comparison, a composite blackbody curve (solid line) has been drawn in, which is a linear combination of curves for temperatures of 3000 and 1000 °K, with coefficients of 0.35 and 0.65, respectively. The scaling of the composite curve was adjusted to give the best visual fit to the data. This is not intended to suggest that our spectrum is produced by two populations of hot particles, one at 1000 and the other at 3000 °K, but rather that the data could be fit very well using a composite curve reflecting a distribution of particle temperatures up to 3000 °K. Furthermore, this spectrum indicates that other sources of light emission, such as charged particle recombination, must make at most a minor contribution to the overall intensity, since the spectrum of such electronic transitions is expected to peak in the UV or visible and to tail off into the IR.[4]

A rough calculation suffices to verify that the temperatures indicated above are reasonable. The temperature of a particle after absorbing energy from a short light pulse is

$$T \approx \frac{3E\phi}{4\pi\rho a C_p \omega^2}, \tag{5}$$

where E is the energy in a single pulse, ϕ the probability of absorption, a, ρ, and C_p the particle radius, density, and specific heat, respectively, and ω the beam spot size. If we model dust as particles of pine charcoal, and take $E = 10^{-5}$ J, $\phi = 0.5$, $\rho = 0.3$ g/cm^3, $a = 2.5 \times 10^{-5}$ cm, $C_p = 0.7$ J/g °K, and $\omega = 10^{-2}$ cm, we obtain $T \approx 2000$ °K. Because the temperature of a particle is proportional to its surface-to-volume ratio, the smallest particles are also the hottest.

The temporal behavior of the light emitted from a predisposed spot with single pulse IR excitation is shown in Fig. 8(a). The sharp rising edge is simultaneous with the arrival of the excitation, and the decay has a time constant of roughly 12 ns. In (b), light emission for the double pulse sequence with 9-ns pulse interval is displayed. In this case the intensity emitted on the first pulse is much smaller than in (a), while

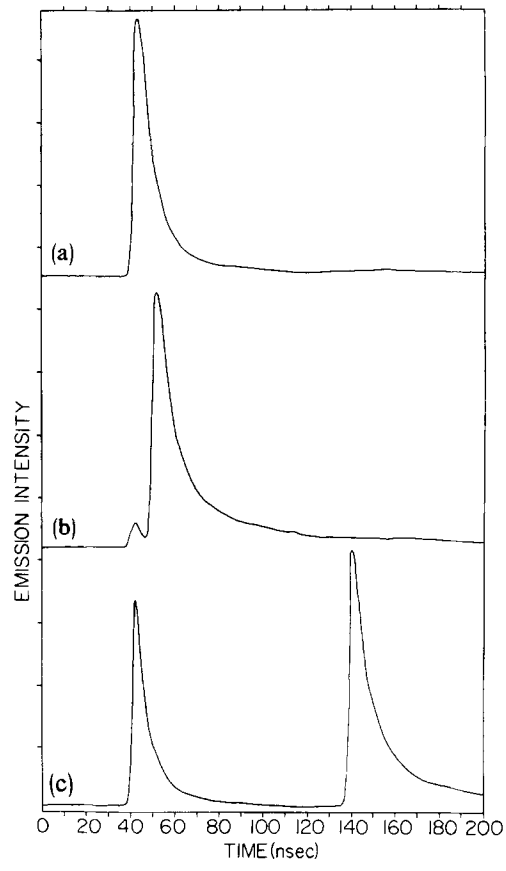

FIG. 8. Time dependence of the visible light emitted by surface particles following three different kinds of excitation: (a) a single IR pulse; (b) a two pulse sequence with 9-ns pulse separation; and (c) a two pulse sequence with 99-ns pulse separation. The emission decay times are approximately constant in each case at ~12 ns. This reflects the particle cooling rates. The amplitude of emission following each laser pulse depends both on the particle temperatures and on the number of particles in the laser spot. Each trace is an average of 200 excitations.

that from the second pulse is comparable. In c is shown the result of increasing the interval between excitation pulses to 99 ns. Now the intensity from the first shot is nearly its value in a, and it is more nearly equal to that from the second shot. Light emitted after the second pulse in the sequence has approximately the same decay rate as that following a single pulse.

If the visible emission from these samples is blackbody radiation from particles having temperatures up to several thousand degrees, then the emission decay must reflect the particle cooling rates. The integrated blackbody intensity for wavelengths up to 1 μm is a strong function of the temperature and has been given by Planck:

$$I = c_1 (e^{c_2/T} - 1)^{-1}, \tag{6}$$

where I is in W/cm^2 of surface), $c_1 = 1\,197\,280$, and c_2 is 28 776. The temperature T at which the intensity falls to $1/e$ of its value at initial temperature T_0 is then

$$T = \frac{T_0}{\left(1 + \frac{T_0}{c_2}\right)}. \tag{7}$$

For $T_0 = 3000$ °K, we obtain $T \approx 2700$ °K. Thus, a tempera-

ture drop of only 10% is sufficient to reduce the emitted intensity by 63%.

It is necessary to show that the temperatures of hot dust particles at the interface can drop by 10% in the observed decay time of 12 ns. The calculation of the average particle temperature as a function of time following the excitation is complicated by the fact that the liquid environment in the immediate vicinity of the particle rapidly increases in temperature and then changes phase. Furthermore, we do not know whether the bubble associated with the hot particle attached to the surface surrounds the particle completely or whether it is in contact at only a point. In order to simplify the problem, we first assume that the liquid remains in thermal contact with the particle during the cooling process, with constant thermal diffusivity κ and particle surface temperature T_s. This gives an upper bound to the cooling rate, since a hot particle surrounded by gas will cool more slowly due to the lower thermal diffusivity of the gas. The average particle temperature is then[14]

$$T_{\rm av}(t) = \frac{6}{\pi^2} \sum_{n=1}^{\infty} \frac{1}{n^2} \left[(T_0 - T_s) e^{-n^2\pi^2\kappa t/a^2} + T_s \right], \quad (8)$$

where T_0 is the initial temperature and a the particle radius. Plots of $T_{\rm av}/T_0$ versus time for various values of a are shown in Fig. 9. Here, we have taken $\kappa = 10^{-3}$ cm^2/s, $T_s = 300$ °K, and $T_0 = 3000$ °K. As expected, the smaller particles cool faster. The effect of increasing the surface temperature T_s from 300 to 600 °K (approximately the boiling point of benzyl benzoate) is shown for the particle with $a = 0.25\,\mu$m. It is small at short times because in either case $T_s/T_0 \ll 1$. It is clear from Fig. 9 that all particles up to a radius of 1 μm can cool to 0.9 T_0 in 10 ns, and the smaller particles, which are hottest and give off the most light, cool much more rapidly, reaching 0.9 T_0 in 5 ns or less. Thus, thermal diffusion is fast enough to account for the emission decay.

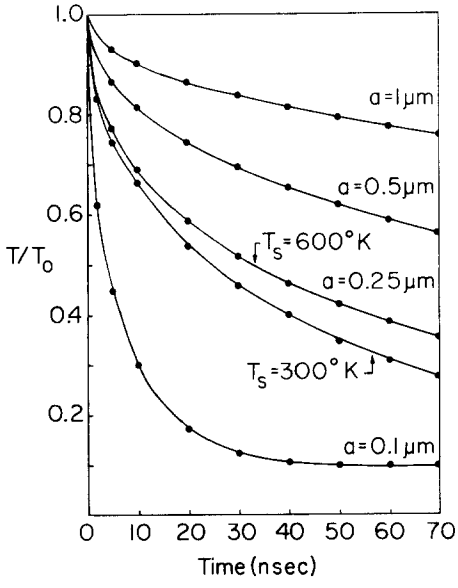

FIG. 9. Rate of cooling of particles of radius a, calculated from Eq. (8) in the text. T is the average particle temperature at time t. The initial temperature T_0 is 3000 °K. The curves are computed assuming the surface temperature T_s is held constant at 300 °K. For comparison, two $a = 0.25\,\mu$m curves are shown, one for $T_s = 600$ °K, approximately the boiling point of benzyl benzoate, and the other for $T_s = 300$ °K. Note that at short times, T is quite insensitive to the value of T_s. The thermal diffusivity κ was taken to be 10^{-3} cm^2/s, appropriate for a liquid. The actual cooling rates will be slower than those shown here, because a particle associated with a bubble will cool more slowly due to the lower thermal diffusivity of the gas.

In view of these results we can understand the important features of light emission for the single and double pulse excitation. With the single IR pulse, particles are accumulated and distributed across the laser spot. Therefore, the light emitted has the appearance of a circular disk under the microscope. With two pulses separated by 9 ns, particles are removed from the center of the spot where the intensity is highest, leaving a ring of particles around the periphery. This accounts for the bright ring of light observed under the microscope, as well as the erasure of the diffraction predisposition. Now when the first pulse arrives, much less light is emitted because particles in the most intense region of the laser spot have been removed. However, after 9 ns, the peripheral particles are still hot ($T \sim 0.5$–$0.9\ T_0$), so that a second IR pulse heats them to a temperature comparable to that reached under single pulse excitation in the center of the spot. This explains the reduced amplitude of emission on the first pulse, and the comparable amplitude on the second [Fig. 8(b)], relative to emission under the single pulse excitation conditions. The fact that the relative intensities of the light emission are more equal for long pulse delays [Fig. 8(c)] indicates that particles heated by the first pulse can cool significantly before the arrival of the second, so that particles are not removed from the surface under these conditions. The latter conclusion is supported by the observation that strong probe diffraction is seen following double pulse excitation for long (~ 100 ns) pulse separations.

These results strongly suggest that there is a temperature threshold for the thermal desorption of particles which is reached by double pulse excitation at small pulse separations. Above this threshold, particles are removed from the surface, causing the diffraction predisposition to be erased and light emission from the center of the irradiated spot to stop. This temperature threshold is not reached either with single pulse excitation or with double pulse excitation with pulse separations long enough to permit significant particle cooling between pulses.

The best evidence that the deposition of surface particles is the origin of both the diffraction predisposition and the light emission is the observation that, if the surface is thoroughly cleaned and the liquid carefully filtered through a pore size of 0.2 μm, no diffraction or light emission can be observed. Subsequent addition of trace amounts of activated charcoal particles to the cleaned liquid regenerates these effects. This demonstrates that the faint dark residue associated with a predisposed spot on the glass surface is not due to processes such as photochemical decomposition of the liquid at the interface, but instead to laser-induced transfer of particles from the liquid to the glass surface.

Thus far there has been no discussion of how the particles become attached to the surface or what the role of the liquid is in this process. Liquids in which these effects were observed include the isotropic phases of *N*-(*p*-cyanobenzylidene)*p*-octyloxyaniline (CBOA) and *p*-*p*'pentylcyanobi-

phenyl, melted benzophenone and biphenyl, triphenyl phosphite, and benzyl benzoate. Those not showing the effects included water, ethyl alcohol, CCl_4, CS_2, benzene, and *n*-hexadecane. Common characteristics of the liquids in the former category are extensive electron delocalization and, with the exception of biphenyl, the additional presence of at least one polar functional group. In view of the well known thermionic emission of laser-heated particles,[2-4] it is reasonable to propose that particles floating near the interface are ionized by the beam. The liquids may serve to stabilize the resulting charge-separated species long enough for the dust to migrate to the glass surface and become attached through electrostatic forces.

This model is attractive because it explains the observed intensity thresholds for particle attachment and removal. The threshold for attachment is the intensity required to raise the temperature of the dust particle sufficiently for ionization to occur. Removal by a double pulse sequence occurs only when the attached particle temperature is raised high enough so that resulting mechanical forces on the particle can overcome the electrostatic forces attracting it to the surface. Without knowing the exact spatial relationships between the hot particle, its associated bubble, and the surface, we can only speculate on the origin of these mechanical forces. Two qualitative observations are relevant. The first is that bubbles leaving the predisposed spot can take particles with them, as evidenced by the dark streak on the glass above the spot. Therefore a model which can account for the efficient ejection of bubbles from the surface could also explain the removal of particles. The second observation is that under single pulse irradiation some microscopic bubbles can be seen through a microscope leaving the surface. However, with double pulse excitation of a single predisposed spot, a tremendous number of microscopic bubbles can be seen leaving during the short time (~ 10 s) prior to the destruction of the predisposition.

One possibility which can account for the particle removal in terms of these observations is illustrated in Fig. 10. In (a) is depicted a dust particle attached to the glass surface. In (b), the first laser pulse of a double pulse sequence arrives, heating the particle and vaporizing a portion of the surrounding liquid. The resulting bubble does not form symmetrically around the particle because it is still attached to the glass surface. In (c) the second laser pulse arrives, heating the particle still more. The particle cools by expanding the existing bubble and by vaporizing additional liquid lying between it and the glass surface. This latter process tends to push both bubble and particle off the surface, as in (d).

One final experimental observation is worth noting. If a fresh spot on the surface of a cuvette containing benzyl benzoate is exposed to grating excitation using one-half of the mode-locked IR pulse train (a sequence of ~ 20 pulses of decreasing amplitude), within 30 s to 1 min we observe damage to the surface of the glass. This is accompanied by the emission of bright, white light, copious bubbles, and an audible hissing sound from the laser spot. Examination of the damaged spot under a scanning electron microscope at $800\times$ magnification revealed that a well-defined diffraction grating had been burned into the glass. In addition, a random network of deep cracks ran throughout the laser spot. The electron micrographs showed no permanent damage to the surface for either the single pulse or double pulse sequence excitation. Most importantly, no damage could be detected after pulse train excitation using liquids which did not exhibit diffraction predisposition or with benzyl benzoate which had been filtered through a pore size of 0.2 μm. These results indicate that the transfer of dust particles from the liquid to the glass surface is an important prerequisite for surface damage in these systems.

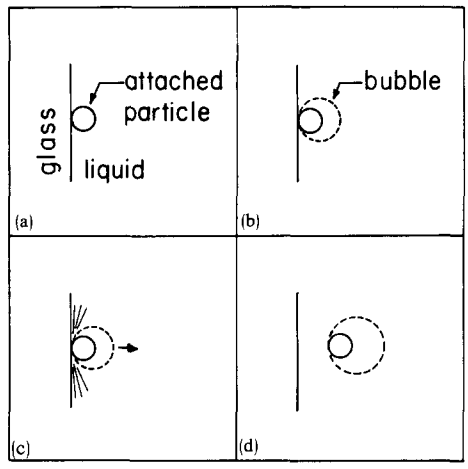

FIG. 10. Possible mechanism for the removal of surface particles by a double pulse sequence. (a) depicts a particle attached to the surface. In (b), the first excitation pulse arrives, heating the particle and vaporizing the surrounding liquid. The resulting bubble does not expand symmetrically around the particle because it is still attached to the surface. In (c), the second pulse arrives, heating the particle still more and vaporizing additional liquid lying between the particle and the surface. If the particle is hotter than a threshold temperature, the force of this latter vaporization is sufficiently large to dislodge the particle and bubble from the surface, as in (d).

IV. CONCLUDING REMARKS

The qualitative, semiquantitative, and quantitative observations reported in this paper describe a diverse but interconnected set of phenomena. We have generated surface diffraction gratings composed of arrays of microscopic bubbles. Although these gratings are only ~ 1 μm thick, they give rise to intense ($\sim 10\%$) diffraction. The diffracted signal was used to measure the time dependence of bubble expansion, contraction, and migration on the surface. Furthermore, we have shown that the bubble gratings are produced following the laser-induced deposition of submicron particles from the bulk liquid onto the surface, and that once deposited, the particles can be removed by an appropriate double pulse sequence. By examining the spectral and temporal characteristics of light emission from the glass surface under various excitation conditions, we have shown that laser heating of the attached particles and their subsequent rapid cooling are intimately involved in these phenomena.

There are several important implications of this work which bear recapitulation. When liquid crystals or ordinary liquids having extensive electron delocalization are studied with laser pulses of $> 10^8$ W/cm^2, special care should be taken to filter the liquid and clean the sample cell in order to

avoid the accumulation of impurity particles at the cell-liquid interface. In addition to causing the emission of light and the production of bubbles, we found that the dust deposited by the laser caused a substantial reduction in the threshold for surface damage.

On the other hand, the ability to manipulate the surface particles using optical beams could lead to some interesting technological applications. For example, one could use a laser beam to deposit surface particles in patterns which could be "read" holographically by beams of lesser intensity through bubble grating diffraction. These patterns could be conveniently erased by an appropriate double pulse sequence, or, if desired, permanently burned into the substrate by a more intense beam. Also, the high efficiency (up to 10% in first order) and fast rise time (~ 350 ps) of the bubble gratings could make them attractive for applications requiring ultrathin, optically activated light switches. Finally, it is likely that magnetic, biological, or chemically reactive particles could be deposited in various patterns on the surface, opening up a range of interesting applications.

ACKNOWLEDGMENTS

G. E. would like to acknowledge the Public Health Service (1 F32 GM08011-01) for a postdoctoral fellowship. We would also like to thank the National Science Foundation (DMR 79-20380) for support of this work. M. D. F. would like to acknowledge the Simon Guggenheim Memorial Foundation for fellowship support which contributed to this research.

[1]Gregory Eyring and M. D. Fayer, Chem. Phys. Lett. **98**, 428 (1983).
[2]D. L. Rousseau, G. E. Leroi, and W. E. Falconer, J. Appl. Phys. **39**, 3328 (1968).
[3]E. M. Logothetis and P. L. Hartman, Phys. Rev. **187**, 460 (1969).
[4]F. Giammanco, A. Giulietti, and M. Vaselli, Opt. Commun. **10**, 46 (1974).
[5]G. A. Askar'yan, A. M. Prokhorov, G. F. Chanturiya, and G. P. Shipulo, Sov. Phys. JETP **17**, 1463 (1963).
[6]G. A. Askar'yan, Sov. Phys. JETP **18**, 555 (1964).
[7]R. C. Stamberg and D. E. Gillespie, J. Appl. Phys. **37**, 459 (1966).
[8]A. A. Manenkov, Sov. Phys.-Dokl. **15**, 155 (1970).
[9]A. A. Chastov and O. L. Lebedev, Sov. Phys. JETP **31**, 455 (1970).
[10]G. A. Askar'yan and T. G. Rakhmanina, Sov. Phys. JETP **34**, 639 (1972).
[11]W. Lauterborn, Appl. Phys. Lett. **21**, 27 (1972).
[12]D. W. Phillion, D. J. Kuizenja, and A. E. Siegman, Appl. Phys. Lett. **27**, 85 (1975); Keith A. Nelson and M. D. Fayer, J. Chem. Phys. **72**, 5202 (1980).
[13]J. R. Salcedo, A. E. Siegman, D. D. Dlott, and M. D. Fayer, Phys. Rev. Lett. **41**, 131 (1978).
[14]H. S. Carslaw and J. C. Jaeger, *Conduction of Heat in Solids* (Clarendon, Oxford, 1959), p. 233.